

# Effect of the deposition time on optical and electrical properties of semiconductor ZnS thin films prepared by chemical bath deposition

O Erken<sup>a</sup>, M Gunes<sup>b</sup>, D Ozaslan<sup>c</sup> & C Gumus<sup>c\*</sup>

<sup>a</sup>Department of Physics, Faculty Science and Letters, Adiyaman University, Adiyaman 02040, Turkey

<sup>b</sup>Department of Materials Engineering, Engineering and Natural Sciences Faculty,  
Adana Science and Technology University, Adana 01180, Turkey

<sup>c</sup>Physics Department, University of Cukurova, Adana 01330, Turkey

*Received 15 July 2016; revised 5 October 2016; accepted 3 January 2017*

Semiconductor ZnS thin films have been deposited by a chemical bath deposition (CBD) on a glass substrate at 80 °C with different deposition time (4, 6 and 8 h). The films have been further studied in order to determine the change in optical and electrical properties as a function of deposition time. The film thicknesses have been calculated between 210 – 1375 nm by using gravimetric analysis. The optical properties of ZnS thin films have been determined by transmittance (%*T*) and absorbance (*A*) measurements by UV-Vis spectroscopy operated wavelength range between 300 and 1100 nm at room temperature. The optical transmittance values of ZnS thin films in the visible region of the electromagnetic spectrum have been found to be between 51–90%. The calculations indicate that the refractive index (*n*) in the visible region is between 1.40 and 2.45. The optical band gaps (*E<sub>g</sub>*) of thin films have been calculated between 3.61–3.88 eV while the band edge sharpness values (*B*) are varied between  $6.95 \times 10^9$ – $8.96 \times 10^{10}$  eV/cm<sup>2</sup>. The specific resistivity values ( $\rho$ ) of the films are found to be between  $1.08 \times 10^5$ – $1.01 \times 10^6$  Ω·cm and exhibit an *n*-type conductivity by Hall measurement.

**Keywords:** ZnS, Thin film, CBD, Optical properties, Electrical properties

## 1 Introduction

Semiconductor zinc sulfide (ZnS) thin films play important role in terms of their utility in optoelectronic and photovoltaic devices. Among II-VI semiconductor compounds, ZnS holds a rather wide band gap (3.8 eV) and a high refractive index (2.3) with an *n*-type conductivity<sup>1-4</sup>. ZnS semiconductor thin films have been recently utilized as a promising materials in applications such as solar panel window materials, information storage, data transfer, and UV-sensitized coatings<sup>5</sup>. The reason of utilizing ZnS in solar panel windows can be explained in terms of having wide band gap of the ZnS electronic structure inducing reduction of absorbance losses, and increasing in the short-circuit current<sup>6</sup>. ZnS thin films show a high refractive index, and have a dielectric filter along with its high transmittance values in the visible region of the light spectrum utilizing them in optical reflector applications<sup>7</sup>. It should be noted that those films can also be used in blue and UV light emitting diode (LED) applications<sup>8</sup>. ZnS thin films require a high

quality growth in order to use them in electroluminescence and solar cell applications. There are various techniques to obtain the high quality of films<sup>9</sup>, such as molecular beam epitaxy<sup>10</sup> (MBE), metal-organic vapor phase epitaxy<sup>11</sup> (MOVPE), metal-organic chemical vapor deposition<sup>12</sup> (MOVCD), pulsed electrochemical deposition<sup>13</sup>, RF magnetron sputtering<sup>14</sup>, hydrothermal<sup>15</sup>, spray pyrolysis<sup>16</sup>, chemical vapor deposition<sup>17</sup> (CVD), and chemical bath deposition<sup>18-20</sup> (CBD). The very fact that the chemical deposition technique is fast, reliable, relatively easy and can also be obtained at high temperatures in atmospheric pressure conditions, which makes it superior to other techniques. Additionally, the technique is suitable for large surface semiconductor coatings with low cost, which can also be taken into account in terms of its advantages over other technique.

In this study, the effects of deposition time on optical and electrical properties of ZnS thin films are deeply investigated by using various experimental techniques. The experimental results showed that ZnS thin films are highly promising materials to utilize the optoelectronic device technology.

\*Corresponding author (E-mail: cgumus@cu.edu.tr)

## 2 Experimental Details

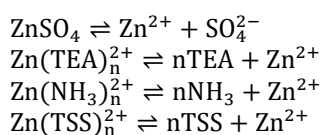
### 2.1 Deposition of ZnS thin films

ZnS thin films are deposited by chemical bath deposition (CBD) on a glass substrate. Prior to the deposition, the glass substrate with dimensions of  $76 \times 26 \times 1 \text{ mm}^3$  is cleaned in a systematical order. The substrate is kept in diluted chromic acid for 5 min, and rinsed in tap water afterwards. Subsequently, the cleaning is further carried out with detergent only to be rinsed again in deionized water (Purelab flex 3, water purity:  $18.2 \text{ M}\Omega$  at  $25^\circ\text{C}$ ). In the last step of the cleaning process, the substrate is kept in ethyl alcohol (99.9% purity) for 10 min and rinsed with deionized water. The drying of the glass substrate is completed in an oven set at  $100^\circ\text{C}$  for 2 h. The chemical constituents and materials for the ZnS thin film processing are selected with great care considering their function in the solutions. The ZnS thin film process solution consists of 1 M  $\text{ZnSO}_4$ , 2.5 mL  $\text{NH}_3/\text{NH}_4\text{Cl}$  buffer solution ( $\text{pH}=10.7$ ), 0.8 mL 0.66 M  $\text{C}_6\text{H}_5\text{Na}_3\text{O}_7 \cdot 2\text{H}_2\text{O}$  (TSS), 2.5 mL 1 M  $\text{N}_2\text{H}_4\text{CS}$  (thiourea), and 0.5 mL 3.75 M  $\text{N}(\text{CH}_2\text{CH}_2\text{OH})_3$  (TEA) mixed with 12 mL of deionized water. The solutions are then transferred to 25 mL sterilized crucibles in order to start the mixing process. The mixing is achieved using a magnetic stirrer until a point of complete homogenization. In the next step, the clean glass substrates that are specified to particular dimensions as mentioned ( $76 \times 26 \times 1 \text{ mm}^3$ ), are dipped into the solution perpendicularly. This prevents any irregular particle precipitations; thus, maintaining a good quality of thin films. The deposition time is kept at 4, 6, and 8 h for one immersing. The temperature is kept at  $80^\circ\text{C}$  at all times during the process of the thin film production. Subsequent to the immersing process, the films are washed with deionized water followed by a drying process in the air. In order to obtain the optical and electrical characterization of the samples, one of the two sides where there is a thin film deposition observed, is removed with the help of a cotton bud, and rinsed with deionized water. The same drying process is repeated. It should be noted that the moisture conditions are strictly controlled, and the experiments are carried out in a no-moisture atmosphere.

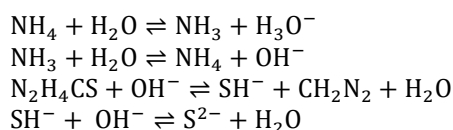
### 2.2 Formation mechanism of ZnS thin films

The selection process for the chemical compounds and materials for the ZnS thin film deposition is handled with care considering their functions and importance in the solutions. TEA [ $\text{N}(\text{CH}_2\text{CH}_2\text{OH})_3$ ] is used in order to prevent the formation of the Zn in the

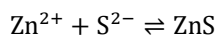
solution; therefore, it reduces the reaction rate. The precipitation speed is slowed down by thiourea ( $\text{N}_2\text{H}_4\text{CS}$ ), which is a moderately acceptable source of sulfides. The utility of TSS ( $\text{C}_6\text{H}_5\text{Na}_3\text{O}_7 \cdot 2\text{H}_2\text{O}$ ) is solely to arrange in solution metallic bonds. However, to maintain a fixed pH value ( $\text{pH}=10.7$ ) ammonia/ammonium chloride ( $\text{NH}_3/\text{NH}_4\text{Cl}$ ) is used as a buffer solution. The function of TEA, TSS and  $\text{NH}_3$  deposition solution is to form a complex compound with ionic zinc followed by a slow release of these complex ions ( $\text{Zn}^{2+}$ ) to the medium. In reference to previous statements, chemical reactions that is necessary to release the  $\text{Zn}^{2+}$  into the medium are given by as follows:



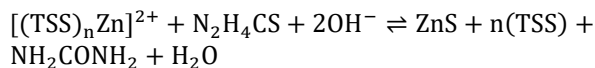
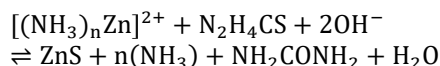
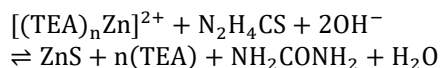
$\text{S}^{2-}$  ions is formed by hydroxylation of ions produced by the buffer solution. The detailed steps regarding the formation of  $\text{S}^{2-}$  are shown below:



$\text{S}^{2-}$  ions are then coupled with  $\text{Zn}^{2+}$  ions to form ZnS as seen in the simple reaction below:



The formation characteristics and reactions of the ZnS from the aforementioned ligands (TEA,  $\text{NH}_3$  and TSS) are given below:



### 2.3 Characterization of ZnS thin films

The thickness measurements of the thin films are performed by a Denver instrument TP-214 model gravimetric analysis tool that has a sensitivity of 0.1 mg, and capable of weighing loads up to 210 g. The measurements are achieved in a two-step, starting with the measurement of a clean glass substrate, and then a glass substrate combined with the formation of thin film on the surface. The optical properties of the thin

films are then determined by the Perkin Elmer UV-Vis Lambda 2S spectrophotometer in the region of  $\lambda = 300\text{--}1100$  nm wavelength. It should also be mentioned that the UV-Vis analysis is carried out at room temperature to obtain the absorbance ( $A$ ) and optical transmittance ( $T$ ) values. Initially a correction of the sort is made on the substrate and the incident beam/radiation that pass through the glass is normalized in a degree of 100%. With those room temperature optical transmittance values, they are let free of their dependency on the absorbance of substrate material. Specific resistivity measurements of thin films are obtained with Hall measurements at room temperature. The specific equipment utilized for these measurements is an Ecopia Hall effect measurement system HS-3000.

### 3 Results and Discussion

#### 3.1 Optical properties

Thin films deposited by the chemical bath deposition method at  $80^\circ\text{C}$  and 4, 6, and 8 h time durations are measured in terms of their thickness with the gravimetric analysis<sup>21</sup>:

$$t = \frac{m}{A \cdot \rho} \quad \dots (1)$$

where  $m$  is the mass of the thin films in g,  $\rho$  is the density in  $\text{g}/\text{cm}^3$  and  $A$  is the deposition surface area in  $\text{cm}^2$ . It is worth noting that the films thickness is considered as a uniform through the sample, and a constant density value<sup>22</sup> of ZnS is taken as  $4.1 \text{ g}/\text{cm}^3$ . The thickness values of the thin films deposited in 4, 6, and 8 h, are measured as 210, 775 and 1375 nm, respectively. Figure 1 shows the variation of ZnS film thickness as a function of the deposition time. As clearly seen in Fig. 1, the film thickness increases linearly with deposition time. The optical transmittance ( $T\%$ ) and absorbance ( $A$ ) values for the ZnS thin films between  $\lambda = 300\text{--}1100$  nm region are given in Fig. 2(a, b).

The examination of the transmittance and absorbance values yields a correlation between the film thickness and optical transmittance. The results reveal that an increase in the film thickness leads to a decline in the optical transmittance by 51% to 90%. Again, the evaluation of the absorbance values indicates that there is a sharp turn of events in the 300-330 nm region when compared to others as seen in Fig. 2(b), while the deposition time appears to increase the absorbance of the films. The absorbance band edge are initialized at  $\sim 310, 320,$  and  $330$  nm, for 4, 6, and 8 h deposition

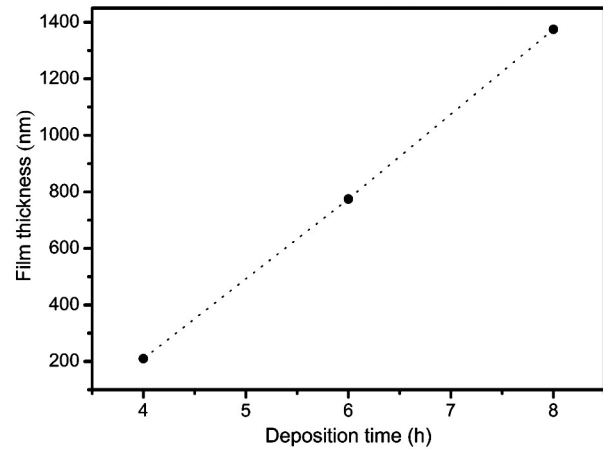


Fig. 1 — Film thickness as a function of the deposition time for 4, 6, 8 h.

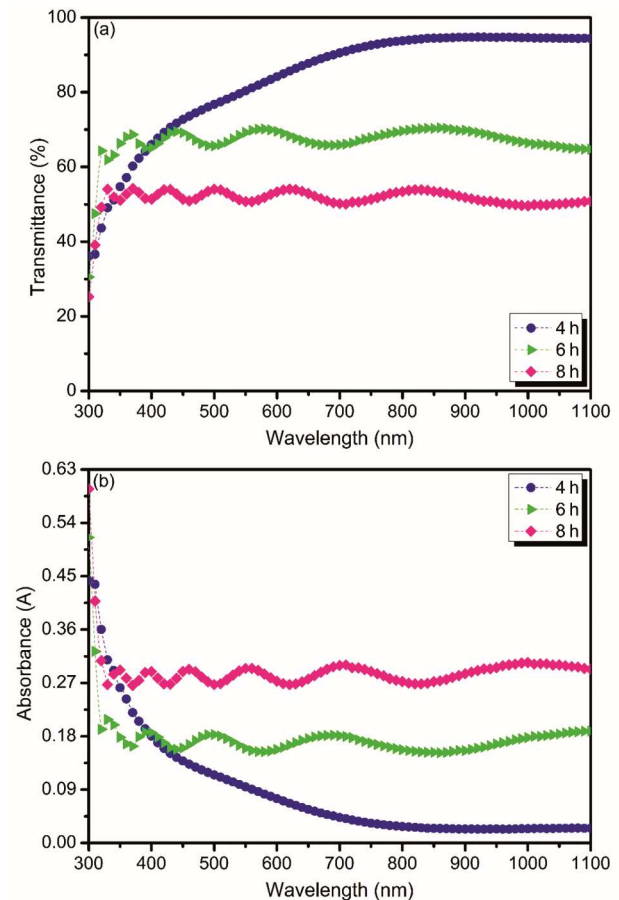


Fig. 2 — Optical (a) transmittance and (b) absorbance spectra of 4, 6 and 8 h samples at  $80^\circ\text{C}$ .

intervals, respectively. It is thought that the offset in the absorption edge is caused by a change in the grain size related to a difference in the film thickness. The different optical property parameters such as the absorption coefficient ( $\alpha$ ), refractive index ( $n$ ), and the

extinction coefficient ( $k$ ) are calculated by using the optical transmittance/absorbance spectrums and equations below<sup>23</sup>:

$$I = I_0(1 - R)^2 e^{-\alpha t} \quad \dots (2)$$

$$T = 10^{-A} \quad \dots (3)$$

$$\alpha = -\frac{1}{t} \ln\left(\frac{I}{I_0}\right) \quad \dots (4)$$

$$R = 1 - \left[ \left( \frac{I}{I_0} \right) e^{\alpha t} \right]^{\frac{1}{2}} \quad \dots (5)$$

$$k = \frac{\alpha \lambda}{4\pi} \quad \dots (6)$$

$$n = \frac{1 + R}{1 - R} + \sqrt{\frac{4R}{(1 - R)^2} - k^2} \quad \dots (7)$$

where  $I$  and  $I_0$  indicate the amount of light that passes through the film and that is received from spectrophotometer, respectively.  $T$  is defined as the optical transmittance.

As clearly seen in Fig. 3, the deposition time causes an increase in the refractive values due to an increase in the film thickness, and the data from the other measurements such as the optical transmittance and absorbance is also proof regarding the aforementioned deductions. Furthermore, there are various studies in the literature in which the same conclusions have been reached regarding the relationship between those parameters<sup>24-26</sup>. Figure 4(a) indicates that the refractive index ( $n$ ) values for the thin films are between

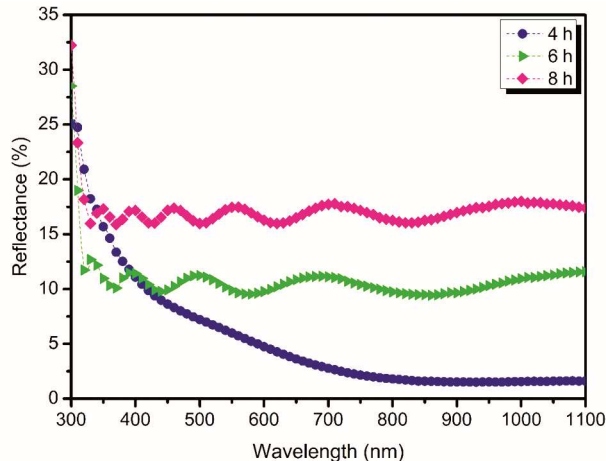


Fig. 3 — Reflection spectra of ZnS deposited for 4, 6, and 8 h at 80 °C.

1.40–2.25, and a rising trend is observed with respect to the increasing deposition time; hence the film thickness. The correlation between the extinction coefficient ( $k$ ) with respect to the wavelength reveals that for the 4 h deposition time, the extinction coefficient decreases as the wavelength increases, whereas for the 6 and 8 h deposition time this relationship exhibits the exact opposite behavior as seen in Fig. 4(b). It can be said that this relationship is expected since the Eq. (6) exposes that there is indeed a correlation between the extinction coefficient ( $k$ ) and absorbance. Additionally, especially upon examination of the Fig. 2(b) spectrum, it can be concluded that there is a dependence of the extinction coefficient on, not only the absorbance, but also the wavelength. The fluctuations over the refractive index ( $n$ ) and extinction coefficient ( $k$ ) are thought to be caused by the grain boundaries within the material structure. It should be pointed out that there is a strong correlation between the results of this study and the literature regarding the relationship between the film thickness and the refractive index<sup>27</sup>:

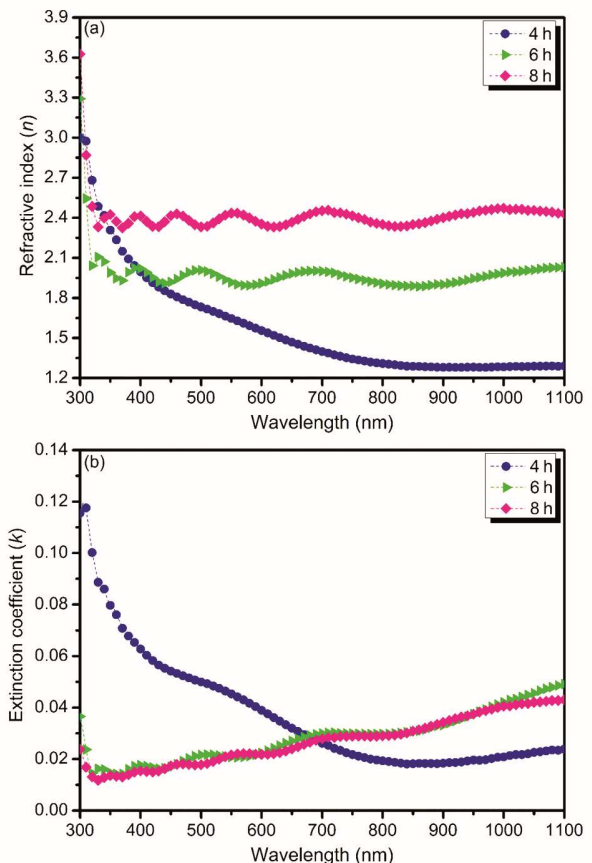


Fig. 4 — (a) Refractive index and (b) extinction coefficient values of ZnS thin films deposited for 4, 6, and 8 h at 80 °C.

$$\varepsilon = \varepsilon_1 + i\varepsilon_2 \quad \dots (8)$$

where  $\varepsilon_1$  is the real dielectric constant and  $\varepsilon_2$  is the imaginary dielectric constant, and the equations for obtaining these values are seen below:

$$\varepsilon_1 = n^2 + k^2 \quad \dots (9)$$

$$\varepsilon_2 = nk \quad \dots (10)$$

The dielectric constant values of the different films are calculated using Eq. (9) for the real dielectric constant ( $\varepsilon_1$ ) and Eq. (10) for the imaginary dielectric constant ( $\varepsilon_2$ ) as demonstrated in Fig. 5(a, b). It is observed in Fig. 5(a) that the real dielectric constant of the thin films increases as the deposition interval widens with the effect of the increasing film thickness. On the other hand, the trend for the imaginary dielectric constant is quite different, as seen previously. The examination of the results reveals that the imaginary dielectric constant values for the 4 h samples decline as the wavelength increases, whereas for the 6 and 8 h samples, the situation is the opposite, since the imaginary dielectric constant climbs as the wavelength

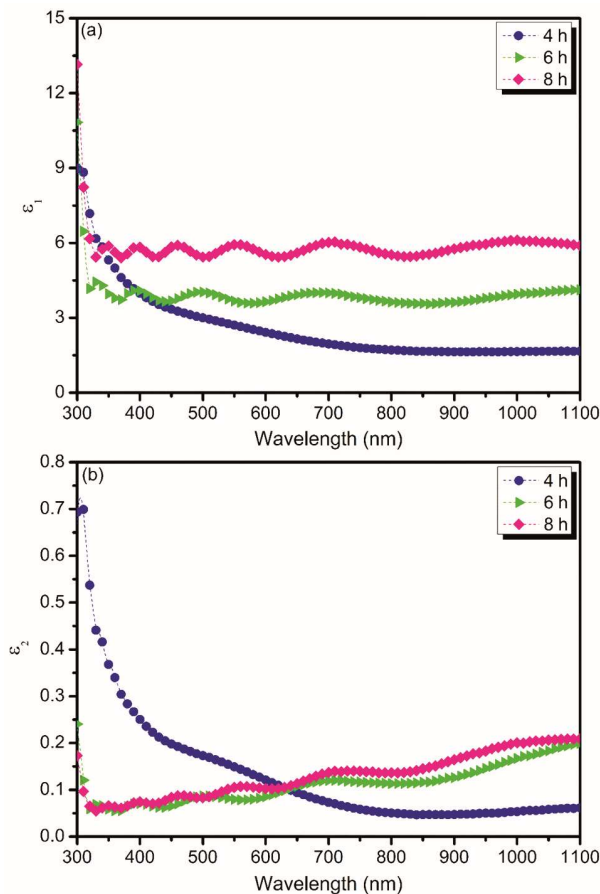


Fig. 5 — (a) Real and (b) imaginary dielectric constant of ZnS thin films deposited for 4, 6, and 8 h at 80 °C.

increases, which is expected given the prior evaluations on these thin films. Equation (9) successfully demonstrates the linear correlation between the refractive index ( $n$ ) and  $\varepsilon_1$  or  $\varepsilon_2$  since the term  $k^2$  is too small to be taken into account where Eq. (10) explains, yet again, the linear correlation between the extinction coefficient and imaginary dielectric constant. It can be said that the analysis from Fig. 4(a,b) indicates the relationship between the wavelength dependent refractive index values and extinction coefficient and real/imaginary dielectric constant analysis, complement to each other. It is worth noting that these results are in full accordance with the literature<sup>28</sup>.

The band gap determinations of the ZnS thin films are obtained by the Tauc equation<sup>29</sup> that is given in Eq. (11):

$$(\alpha h\nu) = A(h\nu - E_g)^n \quad \dots (11)$$

where  $A$  is a constant (number),  $h\nu$  is the energy of a photon particle, and  $E_g$  is the band gap. The value  $n$  indicates a constant number of  $\frac{1}{2}$  for the allowed direct transitions and 2 for the allowed indirect transitions.

The determination of  $E_g$  is accomplished by the determination of the point where  $h\nu$  axis is cut at a point where  $(\alpha h\nu)^2 = 0$  as given in Fig. 6. The band edge

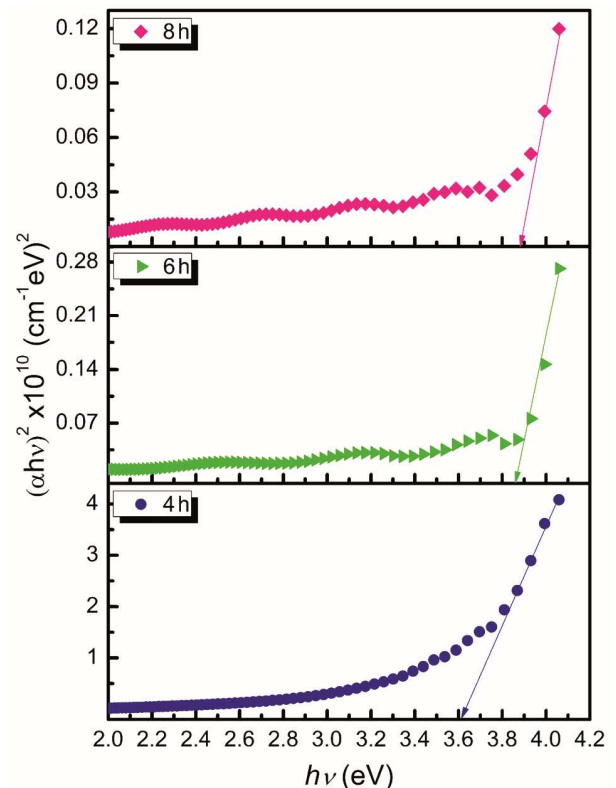


Fig. 6 — Plots of  $(\alpha h\nu)^2$  vs  $h\nu$  for the ZnS thin films deposited at 80 °C with different deposition time (4, 6, and 8 h).

sharpness ( $B$ ) is determined via the slope in the linear region of  $(ahv)^2 - hv$ . Table 1 presents the overview of the optical band gap ( $E_g$ ) and the band edge sharpness ( $B$ ) values.

The values calculated in this section, and given in Table 1, are very much in accordance with the literature<sup>30-33</sup> similar to this study.

### 3.2 Electrical properties

The determination of electrical properties of ZnS thin films is accomplished by an Ecopia Hall effects measurement system HS-3000 tool and all measurements are carried out at room temperature. The values of specific resistivity ( $\rho$ ), mobility ( $\mu$ ) and carrier density ( $n$ ) for ZnS thin films with respect to deposition time is given in Fig. 7. The mathematical correlation between specific resistivity ( $\rho$ ), mobility ( $\mu$ ) and carrier density<sup>34</sup> ( $n$ ) is indicated with Eq. (12):

$$\rho = \frac{1}{ne\mu} \quad \dots (12)$$

The specific resistivity values of the thin films are found to be  $1.08 \times 10^5$ ,  $4.83 \times 10^5$  and  $1.01 \times 10^6 \Omega \cdot \text{cm}$  at  $80^\circ\text{C}$  for 4, 6 and 8 h, respectively. An examination of the values in the literature confirms the values found in this study<sup>35,36</sup>. It should also be noted that the films exhibit an  $n$ -type behavior. It is expected that the time

Table 1 — Variation of  $E_g$  and  $B$  values of the ZnS thin films as a function of the deposition time (4, 6, and 8 h)

Deposition time (h)	Optical band gap $E_g$ (eV)	Band edge sharpness $B$ ( $\text{eV}/\text{cm}^2$ )
4	3.61	$8.96 \times 10^{10}$
6	3.85	$1.17 \times 10^{10}$
8	3.88	$6.95 \times 10^9$

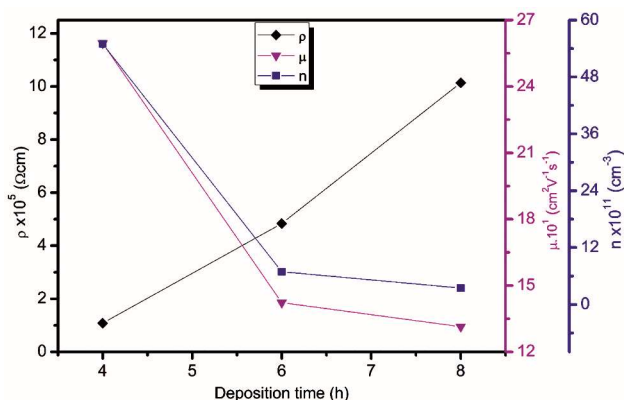


Fig. 7 — Variation of the resistivity, mobility and carrier concentration values of the ZnS thin films as a function of the deposition time (4, 6 and 8 h).

of the film deposition affects parameters such as specific resistivity ( $\rho$ ), mobility ( $\mu$ ) and carrier density ( $n$ ) in a way in which these parameters reduce as the deposition increases, and Eq. (12) is a substantial proof regarding the mathematical background of this behavior. The expectation is satisfied as seen in Fig. 7.

### 4 Conclusions

The production of ZnS semiconductor films is deposited by the chemical deposition in different deposition time such as 4, 6, and 8 h, at  $80^\circ\text{C}$ . The films are then characterized and evaluated in terms of their optical and electrical properties. The film thicknesses are measured to be between 210–1375 nm and it is clearly shown that the film thickness rises up as the deposition time increase. It is also shown that the thin films have a high refractive transmittance ( $T\%$ ), and these values decline as the deposition time extends. The refractive index ( $n$ ) in the visible region of the light spectrum is determined to be between 1.40 and 2.45, and these values show a tendency to increase with rising deposition time. The band gap energy ( $E_g$ ) values vary between 3.61 and 3.88 eV, whereas the band edge sharpness ( $B$ ) values are ranged within  $6.95 \times 10^9 - 8.96 \times 10^{10} \text{ eV}/\text{cm}^2$ . The specific resistivity ( $\rho$ ) values are determined by Hall measurements, and the results indicate that the specific resistivity ( $\rho$ ) for the thin films fluctuate within  $1.08 \times 10^5 - 1.01 \times 10^6 \Omega \cdot \text{cm}$  showing an  $n$ -type conductivity. The thin films produced at  $80^\circ\text{C}$  in different deposition time are adequate candidates for photovoltaic solar panel windows and light emitting diode (LED) applications due to their optical and electrical properties. They can also be utilized in optical applications as such reflectors, as films possess a high refractive index.

### Acknowledgment

This work was supported by Cukurova University under FEF2012D9 project number.

### References

- Manjulavalli T E & Kannan A G, *Int J Chem Tech Res*, 8 (2015) 396.
- Rezagholipour D H, Jamshidi Z A & Ehsani M H, *Chalcogenide Lett*, 8 (2011) 231.
- Cheng J, Fan D, Wang H, Liu B, Zhang Y & Yan H, *Semicond Sci Technol*, 18 (2003) 676.
- Nabiyouni G, Sahraei R, Toghiani M, Majles Ara M H & Hedayati K, *Rev Adv Mater Sci*, 27 (2011) 52.
- Liu J, Wei A & Zhao Y, *J Alloys Compd*, 588 (2014) 228.
- Lopez M C, Espinos J P, Martin F, Leinen D & Ramos-Barrado J R, *J Cryst Growth*, 285 (2005) 66.
- Fathy N, Kobayashi R & Ichimura M, *Mater Sci Eng B*, 107 (2004) 271.

- 8 Antony A, Murali K V, Manoj R & Jayaraj M K, *Mater Chem Phys*, 90 (2005) 106.
- 9 Luque P A, Salas Villasenor A, Quevedo-Lopez M A & Olivias A, *Chalcogenide Letters*, 11 (2014) 105.
- 10 Tomomura Y, Kitagawa M, Suzuki A & Nakajima S, *J Cryst Growth*, 99 (1990) 451.
- 11 Yamaga S, *Phys B*, 185 (1993) 500.
- 12 Sallet V, Lusson A, Rommeluere M & Gorochov O, *J Cryst Growth*, 220 (2000) 209.
- 13 Hennayaka H M M N & Lee H S, *Thin Solid Films*, 548 (2013) 86.
- 14 Hwang D H, Ahn J H, Hui K N, Hui K S & Son Y G, *Nanoscale Res Lett*, 7 (2012) 26.
- 15 Tang C, *J Exp Nanosci*, 9 (2014) 161.
- 16 Elidrissi B, Addou M, Regragui M, Bougrine A, Kachouane A & Bernede J C, *Mater Chem Phys*, 68 (2001) 175.
- 17 Bessergenev V G, Ivanova E N, Kovalevskaya Y A, Gromilov S A, Kirichenko V N, Zemskova S M, Vasilieva I G, Ayupov B M & Shwarz N L, *Mater Res Bull*, 30 (1995) 1393.
- 18 Shinde M S, Ahirrao P B & Patil R S, *Indian J Pure Appl Phys*, 49 (2011) 765.
- 19 Shayesteh S F, Kolahi S & Kalandarragh Y A, *Indian J Pure Appl Phys*, 51 (2013) 780.
- 20 Wary G & Sarma P, *Indian J Pure Appl Phys*, 54 (2016) 379.
- 21 Kulal P M, Dupal D P, Lokhande C D & Fulari V J, *J Alloys Compd*, 509 (2011) 2567.
- 22 Oikkonen M, Tuomi T & Luomajarvi M, *J Appl Phys*, 63 (1988) 1070.
- 23 Gode F & Gumus C, *J Optoelectron Adv Mater*, 11 (2009) 129.
- 24 Cheng J, Fan D, Wang H, Liu B, Zhang Y & Yan H, *Semicond Sci Technol*, 18 (2003) 676.
- 25 Ben N T, Kamoun N & Guasch C, *Appl Surf Sci*, 254 (2008) 5039.
- 26 Zhou L, Tang N, Wu S, Hu X & Xue Y, *Phys Proc*, 22 (2011) 354.
- 27 Echendu O K & Dharmadasa I M, *J Electron Mater*, 43 (2014) 791.
- 28 Gode F, Gumus C & Zor M, *J Optoelectron Adv Mater*, 9 (2007) 2186.
- 29 Bhatt R, Bhaumik I, Ganesamoorthy S, Karnal A K, Swami M K, Patel H S & Gupta P K, *Phys Status Solidi A*, 1 (2012) 176.
- 30 Sartale S D, Sankapal B R, Lux-Steiner M & Ennaoui A, *Thin Solid Films*, 480-481 (2005) 168.
- 31 Gode F, Gumus C & Zor M, *J Cryst Growth*, 299 (2007) 136.
- 32 Liu Q, Guobing M & Jianping A, *Appl Surf Sci*, 254 (2008) 5711.
- 33 Ke H, Duo S, Liu T, Sun Q, Ruan C, Fei X, Tan J & Zhan S, *Mater Sci Semicond Process*, 18 (2014) 28.
- 34 Kariper A, Guneri E, Gode F, Gumus C & Ozpozan T, *Mater Chem Phys*, 129 (2011) 183.
- 35 Wook Shin S, Agawane G L, Gil Gang M, Moholkar A V, Moon J H, Hyeok Kim J & Yong Lee J, *J Alloys Compd*, 526 (2012) 25.
- 36 Ubale A U & Kulkarni D K, *Bull Mater Sci*, 28 (2005) 43.